The United Nations University

GEOTHERMAL TRAINING PROGRAMME
Orkustofnun, Grensásvegur 9,
IS-108 Reykjavík, Iceland

Reports 2006
Number 22

GEOCHEMICAL STUDY OF THE XIANYANG LOW-TEMPERATURE GEOTHERMAL FIELD, SHAANXI PROVINCE, CHINA

Wang Wei
CGC Overseas Construction Co. Ltd.
11/F Tower A, Sinosteel Plaza, 8 Haidian Dajie
Haidian District
Beijing 100080
P.R. CHINA
wangwei@cgcoc.com.cn

ABSTRACT

Xianyang geothermal field, located in the Shaanxi province, is characterized by relatively higher temperature and discharge of geothermal water compared to other low-temperature geothermal fields in China. This study involves the application of geochemical methods to estimate the properties of thermal water from Xianyang. Geothermal water from fifteen wells, divided into three groups based on the distance from the North Wei River fault, is classified according to the Cl-SO_4-HCO_3 triangle diagram, as ranging from mature geothermal water to peripheral waters. Quartz and Na/K geothermometers suggest subsurface temperatures in the range of 76-118°C. Some scaling potential is observed for calcite and magnesium-silicates. Application of a mixing model concludes that mixing with colder water is not obvious. The reservoir is responding to increasing utilization, as changes in the chemical content of the fluid are observed without changes in the measured wellhead temperature.

1. INTRODUCTION

Xianyang, one of the oldest cities in the world, is located in Shaanxi province in central China, and is considered the cradle of Chinese civilization. Xianyang city was the capital of China for twelve dynasties over a period of more than 2000 years and the ancient civilization attracts thousands of tourists every year. Today, around 520,000 people live in the urban districts of Xianyang, an area of about 45 km^2.

Xianyang is rich in low-temperature geothermal resources. Water is produced from the Xianyang geothermal field for house heating in the cities of Xianyang and Xingping, and the towns of Wugong, Liquan and Sanyuan. From 1993 to 2005, 24 geothermal wells were drilled in the geothermal field. Figure 1 shows the location of 18 geothermal wells located in the urban districts of Xianyang. The depth of the wells ranges from 1600 to 3558 m and the temperature ranges from 65 to 104°C (Xing et al., 2005). The exploitation and utilization of geothermal resources in the Xianyang geothermal field has obvious economic, social and environmental benefits. The hot water has been used for space heating during the wintertime, as well as for hot tap water, balneology and medical purposes. In the year 2004, the geothermal hot water use in Xianyang reached about 2 million m^3 (Xing et al., 2005).

Several geological papers have been published on the Xianyang geothermal field but information on its geochemistry has been limited. This report includes a review of the geology of the area but the emphasis is on geochemical analysis of 15 fluid samples collected from different geothermal wells.

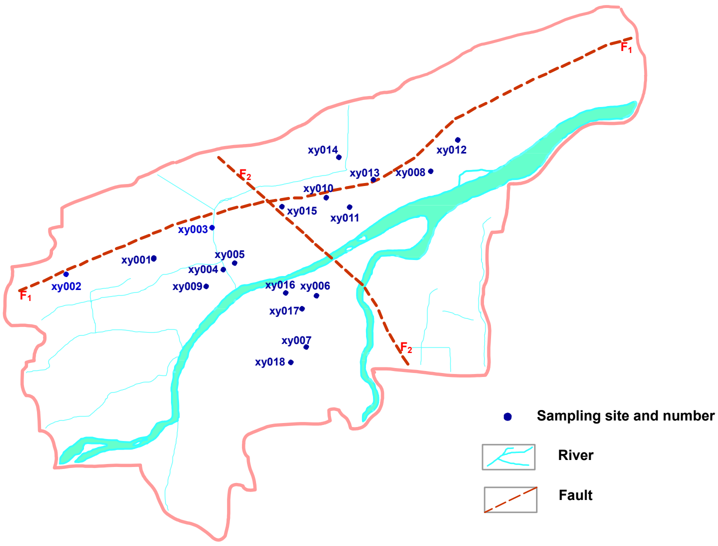

FIGURE 1: Location of the Xianyang wells

2. GEOLOGICAL BACKGROUND

The Xianyang geothermal field is characterized by high temperature and high discharge, strongly affected by the geological structure. The Xianyang geothermal resource is found at depth in the 18,000 km^2 Guanzhong sedimentary basin, which lies to the south of the Yellow River and extends from east to west through the central part of Shaanxi province. This agrees with the information that the water is believed to originate as rain from the slopes of Qinling mountains from several thousand to 30 thousand years ago (Qin et al., 2005). The Guanzhong basin is a Cenozoic fault-block basin filled with extensive Tertiary fluvial, aeolian sediments and Quaternary loess indicated, by geophysical surveys, to range from 3000 to 7000 m in depth (Xing et al., 2005). The basement rock consists of Proterozoic schist and Cenozoic granites (Qin et al., 2005).

The average geothermal gradient of the Guanzhong sedimentary basin is 3.66°C/100 m and it gradually decreases from the southern to the northern area. Anomalies are found in five areas: Baoji, Xianyang-Xinping, Ziwu-zhouzhi, Xi'an-Weinan, and Fuping-Liuqu. The geothermal anomalies of Xianyang-Xinping area are located between the city of Xianyang and Xinping (Xie, 1998). The geological map of the Guanzhong basin shows the Xianyang geothermal field is located in the joint part of the Xianli horst and Xi'an depression between the South Wei River fault and the North Wei River fault (Figure 2). It indicates that the geological structure provides favourable conditions for Xianyang geothermal resources.

The geothermal reservoirs are mainly found in Tertiary sandstones which include four main formations (Figure 3). Overlying are Quaternary sediments with a thickness of around 260 m (Xing et al., 2005). Between the Quaternary and Tertiary formations are clay layers which act as good insulating layers for the deeper reservoirs (Tao, 1995; Tian and Zheng, 1995). The Tertiary formations are:

a) The late Pliocene Zhangjiapo formation with an average thickness of 900 m, composed of alternating layers of mudstone and sandstone with an average porosity of around 26%. Wellhead temperature from this reservoir ranges from 65 to 85°C.
b) The late Pliocene Lantian-Bahe formation with an average thickness of 800 m, composed of layers of mudstone and sandstone with an average porosity of around 24%. This formation is the most productive and wells tapping it produce water of about 80-110°C.
c) The Early Pliocene Gaoling formation with an average thickness of 350 m. It consists of layers of mudstone and sandstone with an average porosity of around 21% and its reservoir temperature is between 80 and 120°C.
d) Bailuyuan formation, found below them, has even higher temperatures and has been tapped by a limited number of wells in Xi'an.

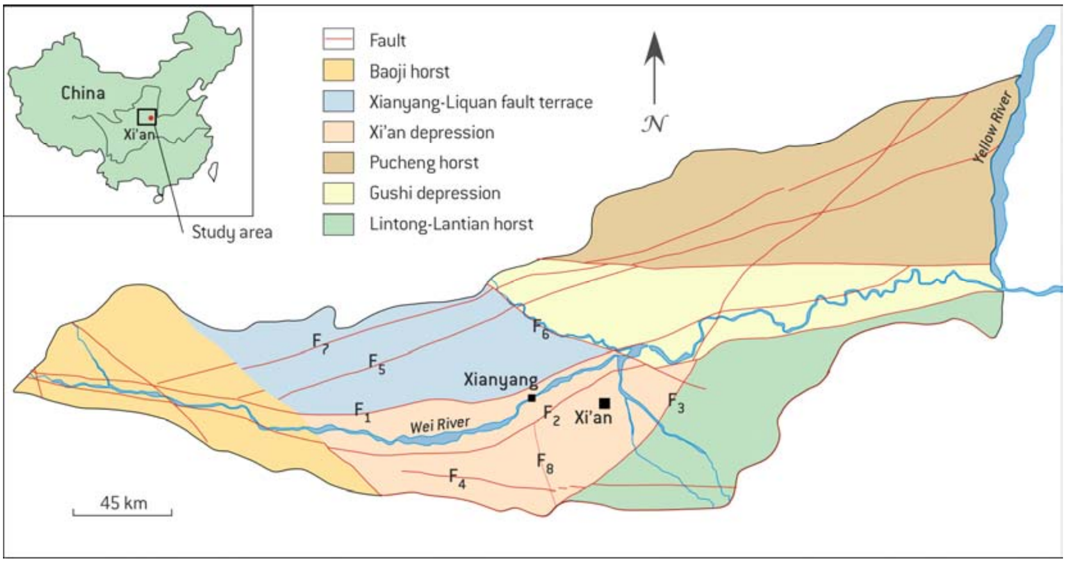

Legend: F_1: North Wei River fault, F_2: South Wei River fault, F_3: Chang´an –Lintong fault, F_4 : Yuxia-Tieluzi fault, F_5: Liquan-Scuanquan-Linyi fault, F_6: Jinghe-Lishan Mountain fault, F_7: Qianxian-Fuping-Yumenkou fault and F_8: Feng River fault.

FIGURE 2: A simplified geological map of the Guanzhong sedimentary basin (Axelsson and Ármannsson, 2005)

There are also indications that carbonate sedimentary rocks exist at depth north of the North Wei River fault. Of the fifteen geothermal wells represented in this paper, five produce from the Zhangjiapo formation, seven from Lantian-Bahe and three from a mixture of the Lantian-Bahe and Gaoling formations, respectively.

In general, the faults and fractures play a multiple role in geothermal activity: (a) They may provide channels for the up-flow of hot water and link to the deeper heat source, as is believed to be the case with the North Wei River fault; (b) The permeability of the reservoir is strongly affected by active faults and fault intersections; (c) Faults may even act as vertical aquifers. As mentioned above, some of the big faults and fractures crossing the Guanzhong Basin play a key role in the geothermal activity in Xianyang, where the North Wei River fault is believed to be the most important. In addition, the geothermal field is divided into two parts by the North Wei River fault, northern and southern areas, with the geothermal resources in the southern area having a higher potential.

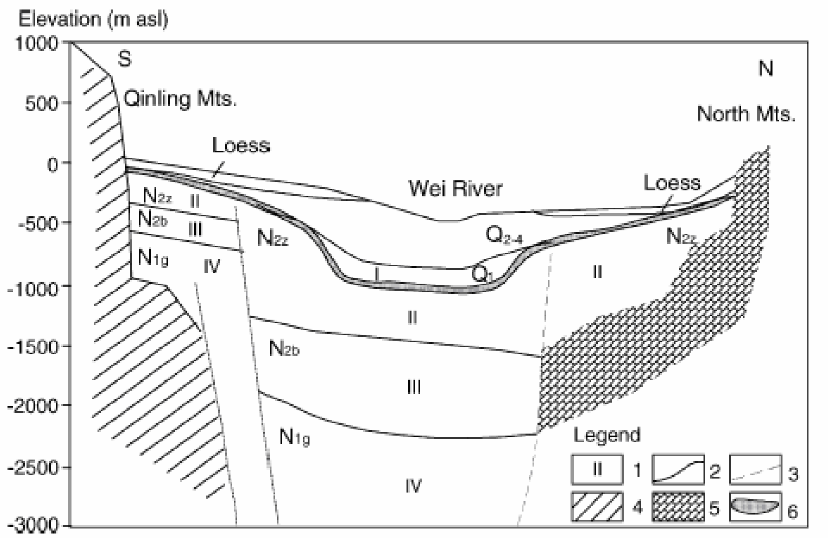

Legend: (1) Geothermal reservoir number; (2) Stratigraphic contacts; (3) Inferred faults; (4) Proterozoic metamorphic rocks; (5) Ordovician-carbonates; (6) Clay layer (aquitard) between Quaternary and Tertiary aquifers; $Q_{2\text{-}4}$: Late Quaternary alluvial deposits; Q_1: Early Quaternary alluvial deposits; N_{2z}: Late Pliocene Zhangjiapo Formation; N_{2b}: Late Pliocene Lantian-Bahe Formation; N_{1g}: Early Pliocene Guoling Group

FIGURE 3: Schematic N-S cross-section of the Guanzhong Basin (Qin et al., 2005)

Minerals identified in the reservoir rocks include analcime, Na-feldspar, calcite, dolomite, quartz, clinochlore, fluorite, muscovite, chalcedony, goethite, anhydrite, chrysotile, and montmorillonite (Tian and Zheng, 1995).

3. CHEMICAL CHARACTERISTICS OF THE GEOTHERMAL FLUIDS

Chemical techniques are applied to determine the characteristics of geothermal fluids, to predict reservoir temperatures, scaling and corrosion tendencies, to obtain information on the origin of the geothermal fluids, and to understand the quality of the geothermal fluid for the intended use (Arnórsson, 2000a).

3.1 Sampling and analysis

The geochemical study for this project is based on samples collected from fifteen geothermal wells by the Bureau of Land and Natural Resources in Xianyang in 2005, as well as information from drilling reports. All samples were analyzed for their total chemical composition, and the analysis was carried out by the Testing Center for Soil and Water, Shaanxi Engineering Prospecting Institute (Table 1). Measurements of pH were performed at 28°C in the laboratory.

TABLE 1: Analytical methods for elements

Element	Method of analysis
Na	Flame photometry
K	Flame photometry
Ca	Titration with EDTA
Mg	Titration with EDTA
CO_2	Titration with HCl using pH-meter
SO_4	Titration with benzidine chloride
Cl	Mohr titration with $AgNO_3$
F	Colorimetric with zirconium alizarin
B	Colorimetric with quinalizarin
SiO_2	Colorimetric with ammonium molybdate
Fe	Atomic absorption spectrophotometry
Al	Atomic absorption spectrophotometry
H_2S	Iodine addition & back-titration with $Na_2S_2O_3$
pH	pH-meter

3.2 Analytical results

The geothermal water is clear and nearly colourless and odourless. The maximum temperature measured at the wellhead is 104°C (well XY009) and the minimum is 65°C (well XY004). Table 2 shows the results of analytical measurements of water from Xianyang wells. The Xianyang geothermal fluid is characterized by pH values from 7.3 to 8.3 and the total dissolved solids (TDS) range from 1703 to 8648 mg/l. The most abundant major ions are Na, Ca, Mg, Cl, HCO_3 and SO_4. The concentration of Na ranges from 485 to 3000 mg/l and for other cations, such as the Ca and Mg, the concentration is lower. The concentration of chloride ranges from 205 to 4502 mg/l. Most heavy metals were below detection limits of the analytical methods used.

The samples are divided into three groups based on the geographical location of the wells in relation to

TABLE 2: Analytical results for major chemical components of geothermal water in the Xianyang geothermal field (mg/l)

Well No.	XY001	XY002	XY003	XY004	XY005	XY006	XY007	XY009	XY010	XY011	XY012	XY013	XY014	XY015	XY017
K^+	39.5	31.5	44	6.25	13	24	4.85	19	42.2	42.2	48.2	85	54.5	25	10
Na^+	2425	2325	2975	630	750	1176.8	485	870	1925	1925	2475	1850	3000	2362.5	705
Ca^+	79.2	96.2	142.3	7	8	20	2.6	12.4	71.1	67.5	98.2	82.2	165.3	102.2	8.4
Mg^{2+}	13.4	26.7	42.8	26.7	33.4	1.8	0.2	1	15.2	12.5	26.1	16.6	47.4	24.9	0.4
NH_4^+	1.4	0.68	0.76	0.72	0.52	0.76	0.38	0.48	0.48	0.56	0.44	1	0.38	1.4	0.34
Fe	3.4	2.4	1.6	0.168	0.216	0.088	0.08	0.376	0.152	0.2	6	0.67	5	0.845	0.256
HCO3	280.7	219.7	216.6	958	674.2	1189.9	585.8	1015.9	387	436.3	295.9	353.9	231.9	310.6	916.5
Cl^-	3332.3	3296.8	4165.4	267.6	584.9	244.6	205.6	242.8	2587.8	2552.4	3598.2	2570.1	4502.2	3172.8	246.4
SO_4^{2-}	547.5	598.9	845.3	237.7	326.6	1296.8	276.2	718	425.1	427.5	391.4	438	610	511.5	429.6
F^-	2.75	2.34	2.19	6.76	6.02	5.62	8.7	5.62	2.4	2.24	295.9	2.04	1.99	2.19	6.72
SiO_2	34.8	31.4	29.8	40.2	63	71.5	59.5	60	47.9	55.5	43.2	54	30.2	46	66.4
Al	<0.01	<0.01	<0.01	<0.01	<0.01	<0.01	<0.01	<0.01	<0.01	<0.01	<0.01	<0.01	<0.01	<0.01	<0.01
CO_2	209.1	162.9	162.8	691.0	486.3	862.7	422.5	732.8	283.5	321.3	217.8	259.7	171.7	280.3	678.7
H_2S	0	0	0	0	0	0	0	0	0.1	0	0	0	0	0	0.1
Li	0.76	0.51	0.77	0.09	0.2	0.68	0.09	0.4	0.65	0.8	0.65	1.01	0.94	1.01	0.312
Sr	14.8	16.5	27	0.08	0.29	0.3	0.05	0.21	9.4	9.45	14.2	14.5	27.6	21	0.88
HBO_2	158	76	124	114	61.5	316	50.5	254	183.5	246	218	252.9	143	184	132.5
TDS	6964.4	6725.9	8468.3	2335	2429.1	4235	1702.9	3364	5541.8	5574.2	6872	5941	8336	6851.3	2603.3
pH	7.6	7.6	7.5	8.3	8.2	7.3	8.2	8.2	7.5	7.3	7.6	8	7.6	7.4	7.5
T	65	68	72	65	96	102	92	104	90	98	91	94	73	89	80
Depth (m)	1600	1600	1751	1958	2583	2800	2653	2995	2471	3100	2976	3558	2000	2813.2	2128

the Wei River and the North Wei River fault. The first group contains samples from wells closest to the fault, the second group includes samples from wells in the area from the northern side of Wei River to the southern side of the fault, and the third one samples taken from the area south of Wei River (Table 3). Figure 4 shows that total dissolved solids (TDS) have a negative linear relationship with the distance to the North Wei River fault, indicating the importance of the fault on the chemical composition of the water. Figure 5 shows that samples in the first group are of the Na-Cl type water with the concentration of chlorine varying from 205 to 4502 mg/l. With distance from the North Wei River fault, the chloride concentration decreases, but the HCO_3 and SO_4 concentrations increase. Accordingly, the water types of groups II and III are mainly Na-HCO_3-Cl, Na-HCO_3-SO_4 and Na-SO_4-HCO_3. Proximity to the fault seems to have more influence on the chemical composition than does the well depth.

TABLE 3: Groups of wells

Group	Well no.
I	XY001, XY002, XY003, XY010, XY011, XY012, XY013, XY014, XY015
II	XY004, XY005, XY009
III	XY006, XY007, XY017

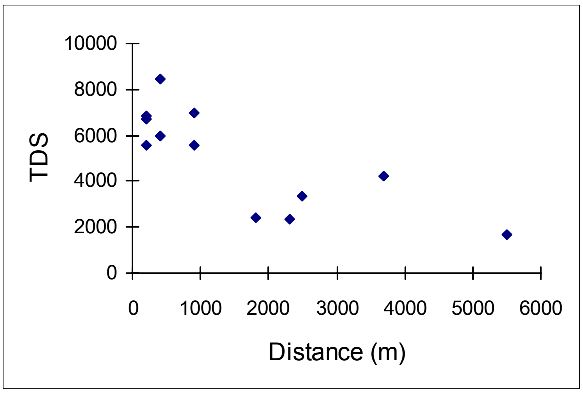

FIGURE 4: TDS versus distance from North Wei River fault

3.3 Classification of the thermal fluids

Before further interpretation of chemical analysis, it is useful to carry out an initial classification of the water samples. The Cl-SO_4-HCO_3 triangular diagram is one of the diagrams used for classifying natural waters, based on the relative contents of three major anions: Cl, SO_4 and HCO_3 (Giggenbach, 1991). In this diagram, composition ranges are indicated for several groups of water such as volcanic and steam-heated water, mature water and peripheral water. Furthermore, this diagram may provide initial indications of mixing relationships or groupings. According to Giggenbach (1991), solute geothermometers can only be applied to what is referred to as "mature water", characterized by high Cl and low SO_4, making it possible to weed out samples that are not suitable for solute geothermometer analyses.

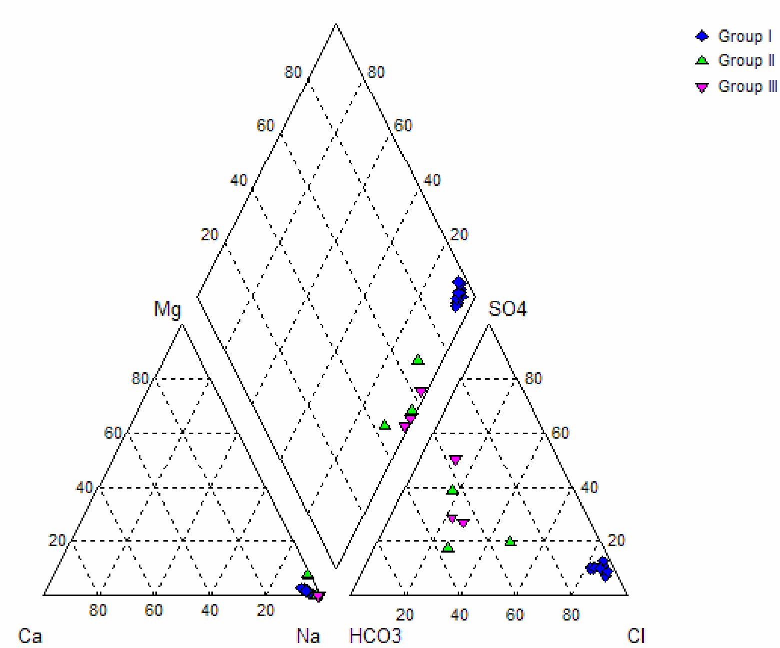

FIGURE 5: Piper diagram showing chemical types of Xianyang thermal water

In order to plot data points in such a triangular plot, the first step is to obtain the sum S of the concentrations of all three constituents involved, as follows:

$$S = C_{Cl} + C_{so_4} + C_{HCO_3}$$

where C is the concentration in mg/l.

Then, the percentage concentration for each of the three constituents is calculated. The results of calculations for the geothermal waters in Xianyang are presented in Figure 6. The samples from group I plot in the area close to "mature geothermal water" and are classified as those of Cl-rich geothermal water with neutral pH, which geochemical techniques can be applied to with confidence. The samples from groups II and III fall in the bicarbonate area close to peripheral waters. This indicates that the samples from groups II and III are possible mixed with cold groundwater or the higher HCO_3 concentration of the water is a result of the presence of carbonate rocks. Considerable caution is required for applying most geoindicators for the samples from these two groups.

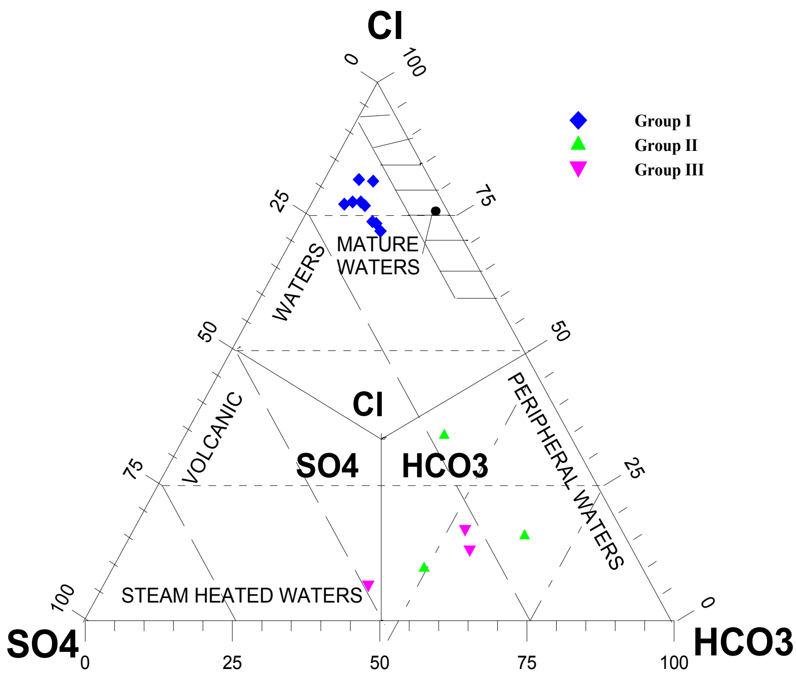

FIGURE 6: Cl-SO_4-HCO_3 diagram for the Xianyang thermal water samples

3.4 Chemical geothermometers

One of the most important applications of geochemistry for geothermal resources is using chemical geothermometers to predict subsurface temperatures and give valuable information about what is happening in the reservoir. The accuracy of a geothermometer application is based on two assumptions. The basic assumption is that a temperature-dependent equilibrium is attained between fluid and minerals in the reservoir. It is further assumed that the composition of a fluid is not affected by chemical reactions in the upflow of geothermal system zones where cooling occurs.

Many water geothermometers were developed from the mid-1960s to the mid-1980s. The most important ones are silica (quartz and chalcedony), Na/K and Na-K-Ca geothermometers. However, when applied to the same fluid, various geothermometers frequently yield different values for reservoir temperatures due to a lack of equilibrium between the solution and hydrothermal minerals, or as a result of reactions, mixing or degassing during upflow (Tole et al., 1993).

3.4.1 Silica geothermometers

The two main types of temperature-dependent reactions that may be useful as quantitative geothermometers are solubility and exchange reactions. At depth, generally attained by commercial drilling for geothermal resources, variations in pressure and added salt have little influence on the solubility of silica. Based on the above conditions, the dissolved silica concentration in a hydrothermal solution can generally be used as one of the more reliable chemical geothermometers. The silica geothermometers, used at present to predict subsurface temperatures of reservoirs, are based on experimentally determined solubilities of chalcedony and quartz.

Since there are various silica minerals with different solubilities, it should be known which silica mineral is controlling the dissolved silica concentration when using the silica geothermometers. It means that different silica geothermometers are valid at different temperatures. In general, the quartz geothermometer works well in high-temperature reservoirs, but the chalcedony geothermometer is better for low-temperature reservoirs. The reason is that at low temperatures, the rate of quartz precipitation does not cope with the rate of silica release into solution by dissolving primary minerals; on the other hand, chalcedony is unstable at temperatures above 120-180°C. However, in mature sedimentary rocks which contain less reactive minerals, despite being a low-temperature field with temperatures less than 100°C, quartz can control dissolved silica. In another situation, chalcedony may control dissolved silica up to temperatures as high as 180°C. Therefore, there is ambiguity in the use of silica geothermometers at temperatures less than about 180°C.

The most widely used formula for the quartz geothermometer is (Fournier and Potter, 1982):

$$T°C = -42.198 + 0.28831 SiO_2 - 3.6686 \times 10^{-7} SiO_2^{\ 3} + 77.034 \log SiO_2$$

Fournier (1977) presented the chalcedony no steam loss geothermometer:

$$T°C = \frac{1032}{4.69 - \log SiO_2} - 273.15$$

where SiO_2 concentrations are in ppm.

3.4.2 Cation geothermometers

Cation geothermometers are based on ion exchange reactions with temperature-dependent equilibrium constants. A typical example is the exchange of Na^+ and K^+ between co-existing alkali feldspars:

$$NaAlSi_3O_8 + K^+ = KAlSi_3O_8 + Na^+$$

Two assumptions are made, that the activities of the solid reactions are unity and the activities of the solid reactions of the dissolved species are equal to their molal concentrations in aqueous solution. The equilibrium constant, K_{eq} for this reaction is:

$$Keq = \frac{[Na^+]}{[K^+]}$$

The equilibrium constant changes with temperature, so it is possible to calculate subsurface temperatures based on the concentrations of these cations in geothermal water.

The *Na/K geothermometer* is based on ion exchange between albite-microcline, albite-adularia or Na-K montmorillonite and water. The reactions on which this geothermometer is based take a longer time to reach a new water-rock equilibrium at a given temperature than those on which other geothermometers are based and estimated (Fournier, 1989). Therefore, compared to a silica geothermometer, the Na/K geothemometer takes a longer time to attain a new water-rock chemical equilibrium during the ascent of a geothermal fluid (Arnórsson, 2000b). The Na/K geothermometer is applied to estimate possible higher temperatures originating in the deeper parts of a system where waters reside for relatively long periods of time. However, it may be slightly disturbed by mixing with cold dilute waters (Fouillac and Michard, 1981).

In order to account for different mineral assemblages and structural states of the minerals from one place to another, many Na/K geothermometer equations have been presented. In this study, the following equations have been used (the concentrations of Na and K are in ppm):

Na/K geothermometer (Giggenbach, 1988):

$$t(°C) = \frac{1390}{1.75 + \log\frac{Na}{K}} - 273.15$$

Na/K geothermometer (Arnórsson et al., 1983a):

$$t(°C) = \frac{933}{0.780 + \log\frac{Na}{K}} - 273.15$$

Na/K geothermometer (Fournier, 1979):

$$t(°C) = \frac{1217}{1.483 + \log\frac{Na}{K}} - 273.15$$

The *Na-K-Ca geothermometer* is based on reactions involving the exchange of Na, K, and Ca with mineral solid solutions and appears to give excellent results for most waters above about 200°C, but erratic results are obtained for waters from reservoirs at less than 200°C. The Na-K-Ca geothermometer is empirically calibrated, different from the silica and Na/K geothermometers. It is not related to equilibrium with specific geothermal minerals (Arnórsson et al., 1983b).

Fournier and Truesdell (1973) presented the equation for Na-K-Ca which has been used in both low-temperature and high-temperature geothermal reservoirs as follows (the concentrations of Na, K, and Ca are in ppm):

$$t(^0C) = \frac{1647}{\log\frac{Na}{K} + \beta\left(\log\frac{\sqrt{Ca}}{Na} + 2.06\right) + 2.47} - 273.15$$

where β = 4/3 when calculated temperature is < 100°C;
β = 1/3 when calculated temperature is > 100°C.

An exception to this rule is that β equal to 1/3 should be used for waters less than 100°C when $\log(Ca^{1/2}/Na)$ is negative, with concentrations of dissolved constituents expressed in molality units.

The *K/Mg geothermometer* is based on the equilibrium between water and the mineral assemblage K-feldspar, K-mica and chlorite (Giggenbach, 1988). Water-rock exchange reactions involving Mg proceed relatively quickly at low temperatures, and a K/Mg ratio appears to be a good indicator of the last temperature of water-rock equilibrium in upflow zones.
K/Mg geothermometer (Giggenbach, 1988):

$$t(°C) = \frac{4410}{14.0 - \log\frac{K}{\sqrt{Mg}}} - 273.15$$

3.3.3 Na-K-Mg triangular diagram

Giggenbach (1988) suggested a triangular diagram with Na/1000, K/100, $Mg^{1/2}$ at the apices to classify waters into fully equilibrated, partially equilibrated and immature waters (dissolution of rock with little or no chemical equilibrium). It is based on the temperature dependency of the full equilibrium assemblage of potassium (K) and sodium (Na) minerals that are expected to form after isochemical recrystallization of an average crustal rock under conditions of geothermal interest. The triangular diagram is also employed to determine whether a fluid has equilibrated with hydrothermal minerals as well as to predict the equilibrium temperatures, $T_{Na\text{-}K}$ and $T_{K\text{-}Mg}$. The value of $T_{K\text{-}Mg}$ is likely to reflect conditions at shallow levels, whereas $T_{Na\text{-}K}$ gives indications at considerable depth (Giggenbach, 1988). In addition, the Na-K-Mg tiangular diagram provides a tool for selecting samples that are suitable for the application of the cation geothermometer.

The use of the triangular diagram is based on the temperature dependence of the three reactions (Giggenbach, 1988):

$$K - feldspar + Na^{+} = Na - feldspar + K^{+}$$

$$2albite + 0.8K - feldspar + 1.6water + Mg^{2+} = 0.8Mica + 0.2chlorite + 5.4silica + 2Na^{+}$$

$$2.8K - feldspar + 1.6water + Mg^{2+} = 0.8Mica + 0.2chlorite - 5.4silica + 2K^{+}$$

The sum is calculated according to:

$$S = \frac{C_{Na}}{1000} + \frac{C_K}{100} + \sqrt{C_{Mg}}$$

where C is in mg/l, in the calculation of the "%C_{Na}/1000", "%C_K/100" and "%$Mg^{1/2}$".

Figure 7 shows that samples from groups II and III plot close to the "fully equilibrated line", suggesting attainment of water-rock equilibrium compared to the samples from group I. Accordingly, geothermometers can be applied to these samples fairly well in order to predict the subsurface temperature. The $T_{Na\text{-}K}$ temperature varies within the range of 70-160°C. The $T_{K\text{-}Mg}$ temperature ranges from 60 to 110°C. In addition, the Mg-concentration of the samples is in fact surprisingly high compared to other analyses from the Guanzhong basin (Ármannsson, 2005).

3.3.4 Application of silica and cation geothermometers

Calculations of subsurface temperatures were done with the aid of the WATCH speciation program using quartz, chalcedony and Na/K (Arnórsson et al., 1983a) geothermometers (Bjarnason, 1994). Calculations of other geothermometers listed in Table 4 were obtained by using different geothermometric equations previously mentioned in Section 3.

TABLE 4: Geothermometer temperatures for thermal waters from the Xianyang geothermal field field

Group	Well no.	$T_{mea.}$	$T_{qtz.}$	$T_{cha.}$	$T_{Na/K(1983)}$	$T_{Na/K(1988)}$	$T_{Na/K(1979)}$	$T_{Na-K-Ca}$	T_{K-Mg}
I	XY001	65	84	53	59	120	99	125	67
	XY002	68	80	49	53	111	90	116	61
	XY003	72	78	46	57	115	94	120	62
	XY010	90	98	68	76	135	114	136	67
	XY011	98	105	75	76	135	114	136	68
	XY012	91	93	93	70	129	108	132	65
	XY013	94	102	71	125	177	158	169	75
	XY014	73	79	47	66	125	104	128	64
	XY015	89	97	66	43	100	79	106	58
II	XY004	65	89	57	42	97	76	104	44
	XY005	96	108	78	65	123	102	128	50
	XY009	104	104	74	75	134	114	137	74
III	XY006	102	118	89	70	131	110	134	73
	XY007	92	105	75	42	98	76	107	67
	XY017	80	114	85	55	113	92	118	71

The wellhead temperatures measured for Xianyang geothermal field are shown in Table 4, ranging from 65 to 104°C. Temperatures estimated by the chalcedony geothermometer ($T_{cha.}$) are generally lower than temperatures estimated by other geothermometers, and are often even lower than measured temperature ($T_{mea.}$). As a result, it is assumed that quartz is controlling the silica phase and the chalcedony is considered unreliable for estimating the subsurface temperature. On the other hand, the Na-K-Ca geothermometer gives the highest temperature, possibly due to calcite precipitation. The results from the three Na/K geothermometers are quite different. It is obvious that the Na/K geothermometer by Giggenbach et al. (1988) yields relatively high values for all samples compared to the other two. The reason is that they are based on different mineral assemblages, and the results depend on which minerals control the mineral-fluid equilibration. There is also a considerable difference between Na/K and K/Mg geothermometers, the latter showing considerably lower temperatures. It is possible that this is because the K/Mg ratio responds faster than the Na/K ratio to changes in temperature. However the difference between estimations of temperature by the two geothermometers decreases with the increasing distance from the North Wei River Fault.

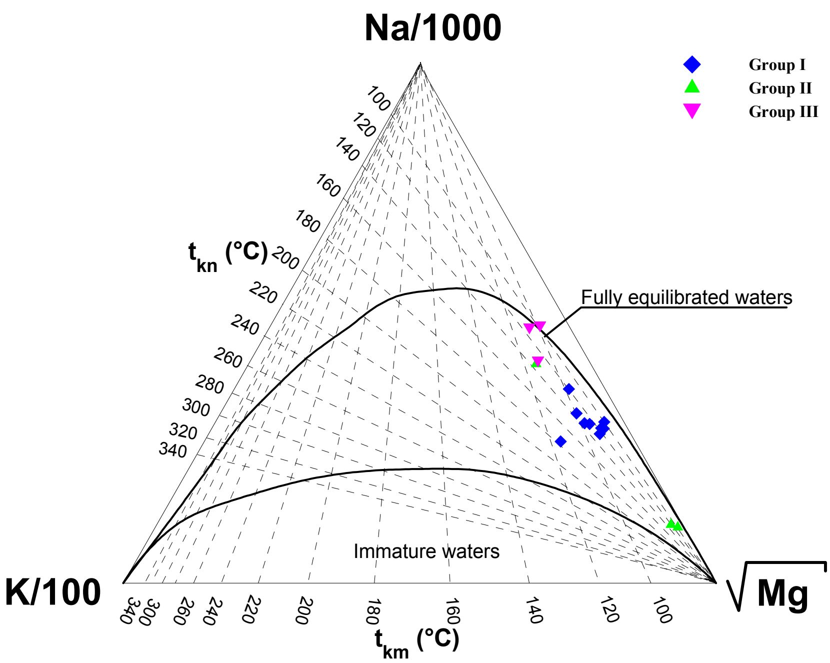

FIGURE 7: Na-K-Mg diagram for the Xianyang thermal water

The quartz ($T_{qtz.}$) (Fournier and Potter, 1982) and Na/K ($T_{Na/K(1979)}$) geothermometers seem to be most suitable for the Xianyang geothermal field, giving similar results. These results indicate that the geothermal fluid has been in contact with ancient sandstone and accordingly the quartz and Na-K geothermometers are most likely to reflect subsurface temperatures in the reservoir. Analyses of geothermometer calculations show that the water in Xianyang geothermal field originates from a low-temperature source where reservoir temperatures may be as high as 120-130°C (Axelsson and Ármannsson, 2005).

3.5 Mineral solution

The application of silica and cation geothermometers is based on the assumption that particular minerals attain equilibrium with the fluids in the reservoir. However, Reed and Spycher (1984) have presented a different approach to geothermometers. This approach involves the evaluation of the saturation state of a specific water composition with a large number of minerals as a function of temperature. The saturation equilibrium state of minerals can be estimated by the logarithm ratio of the ion activity product (Q) to the solubility product (K), called the saturation index (SI), where Q is calculated from analytical results for a water sample and K is the theoretical solubility constant for a specific mineral. If the value of log (Q/K) is equal to zero, the water has reached the saturation equilibrium with respect to a mineral. If a group of minerals is close to equilibrium at one particular temperature, it means the water has equilibrated with this group of minerals and this temperature reflects the temperature of the reservoir. In addition, if the value of log (Q/K) is greater than zero, it indicates that the water is supersaturated and the mineral has a tendency to precipitate, but if it is less than zero, it means the water is undersaturated and the mineral has a tendency to dissolve.

Log Q and log K were calculated by the program WATCH (Arnórsson, et al., 1982; Bjarnason, 1994). As the chemical data from the Xianyang geothermal field did not contain aluminium analyses, six aluminium free minerals were selected for SI calculations: anhydrite, chrysotile, calcite, fluorite, amorphous silica, and quartz. The saturation index was calculated for temperatures between 20 and 120°C. The diagrams (Figure 8) appear to have a similar pattern for most samples and do not show a clear conversion to the zero saturation index by any group of minerals. In other words, the fluid is not in equilibrium with the assumed subsurface mineral assemblage at a certain temperature. The limitation of mineral choices, due to the absence of aluminium analysis data, impacts the results. For some samples (XY006) there is an indication of a pre-existing equilibrium where an intersection for SI for several minerals was shifted downwards. This suggests some degree of equilibrium in the deeper part of the geothermal system.

The saturation index (SI) can be applied for the evaluation of scaling potential. All the samples are slightly undersaturated with respect to anhydrite, amorphous silica and fluorite over the reference temperature range. As a result, the risk of precipitation of those minerals is low. The pattern of the calcite saturation index plots above the zero line in all the diagrams except for XY006, XY007 and XY017, and furthermore, calcite solubility is inversely related to water temperature. For samples containing high Mg content, the Mg-silicate mineral chrysotile represents Mg-bearing clay-like minerals. Although chrysotile plots for some samples as being supersaturated, it is unlikely that chrysotile is precipitating from this water. If the thermal water is heated, it is possible that calcite and minerals similar to chrysotile are likely to cause scaling. As quartz solubility increases with increasing temperature, cooling will cause supersaturation, eventually leading to precipitation. On the other hand, there are some differences between the deeper wells and shallow wells. Samples XY010-XY015 were taken from the deeper wells and are saturated at wellhead temperature for calcite, chrysotile and silica. Samples from shallow wells XY001-XY003 are different. Calcite and chrysotile reached saturation at a temperature close to the wellhead temperature.

No scaling problems have been reported in Xianyang, but if more extensive utilization is planned, reliable chemical analysis and deposition rate experiments are recommended.

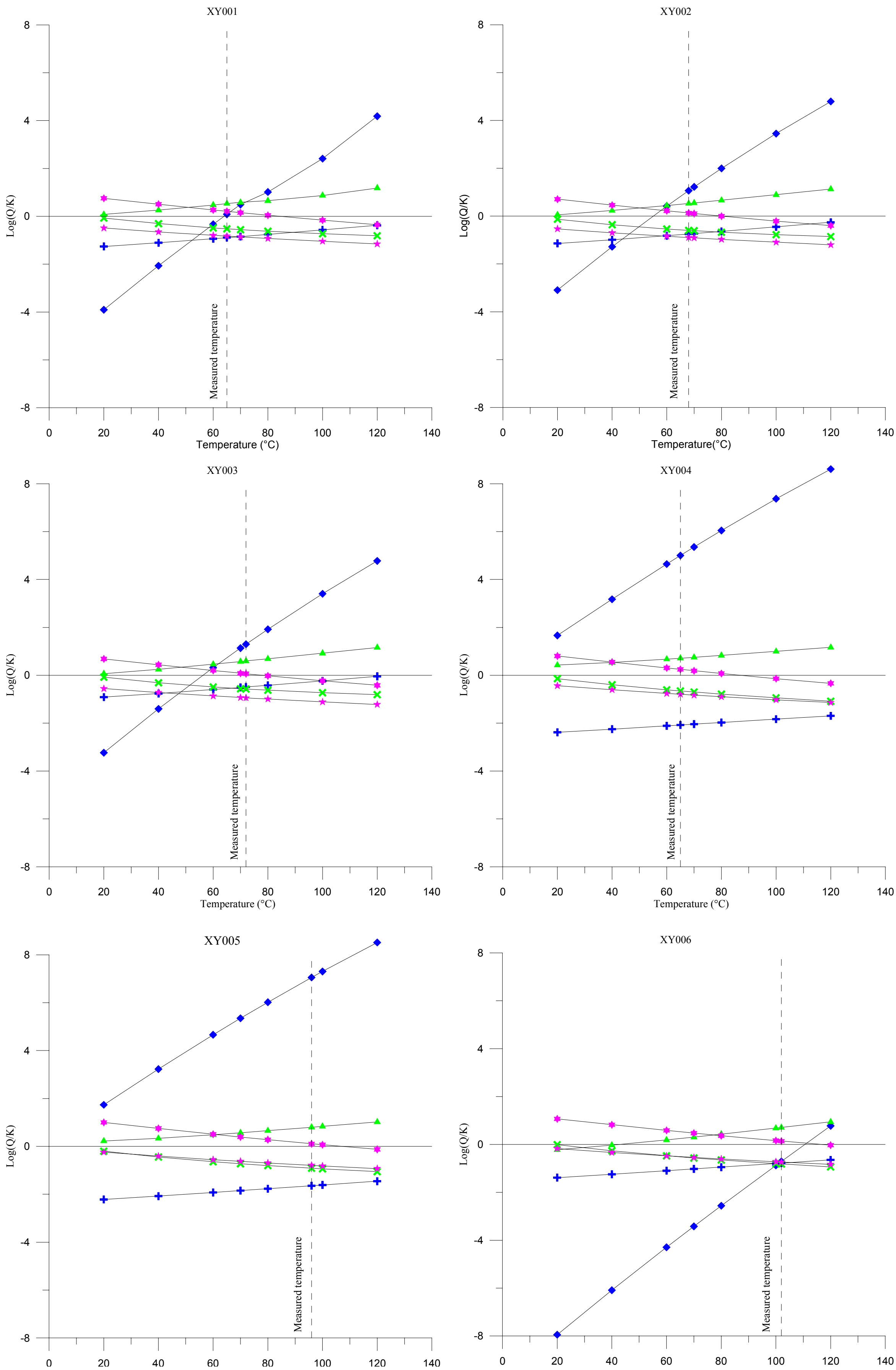

FIGURE 8: Log Q/K diagrams for the Xianyang thermal water samples

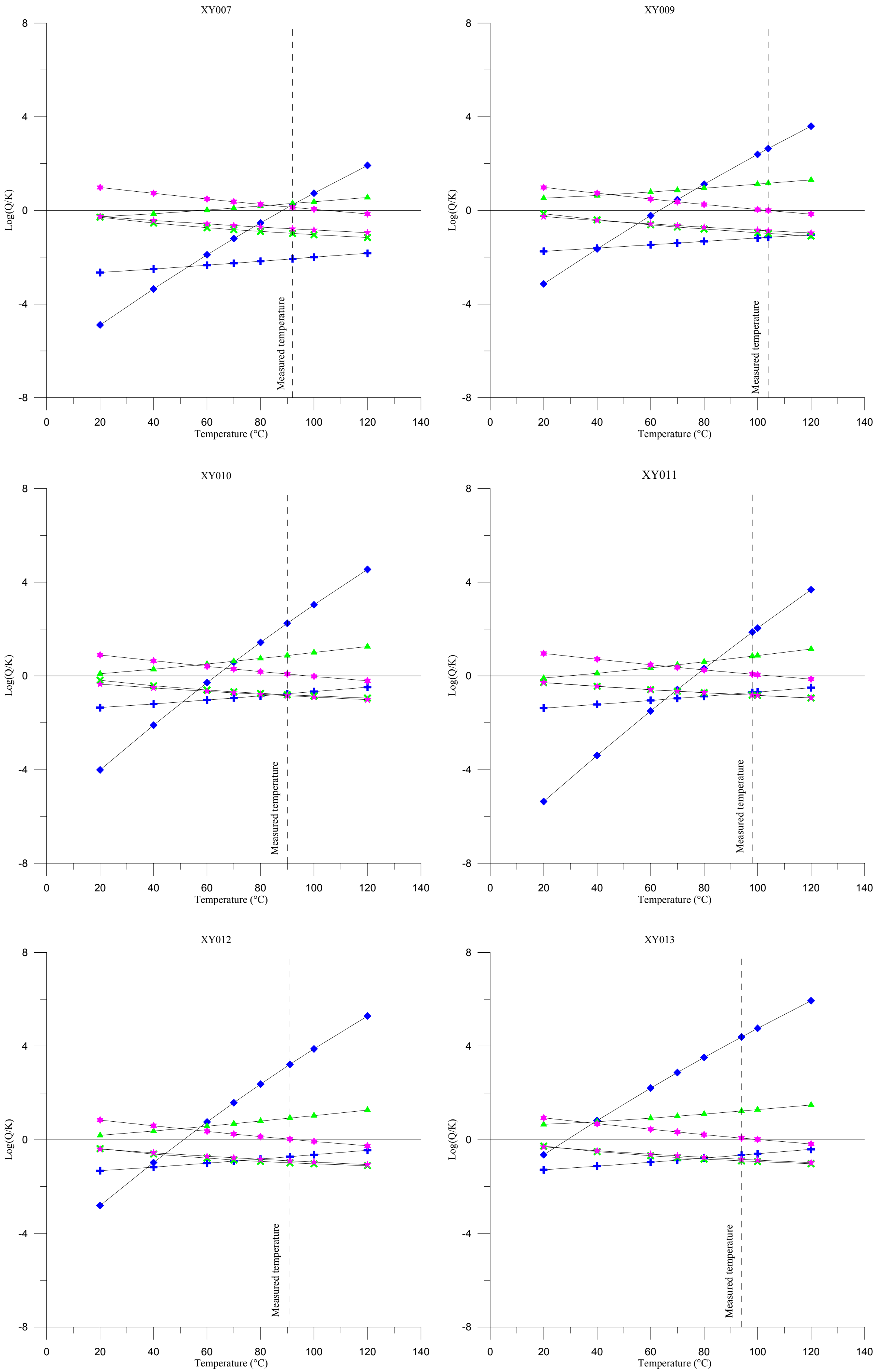

FIGURE 8 continued: Log Q/K diagrams for the Xianyang thermal water samples

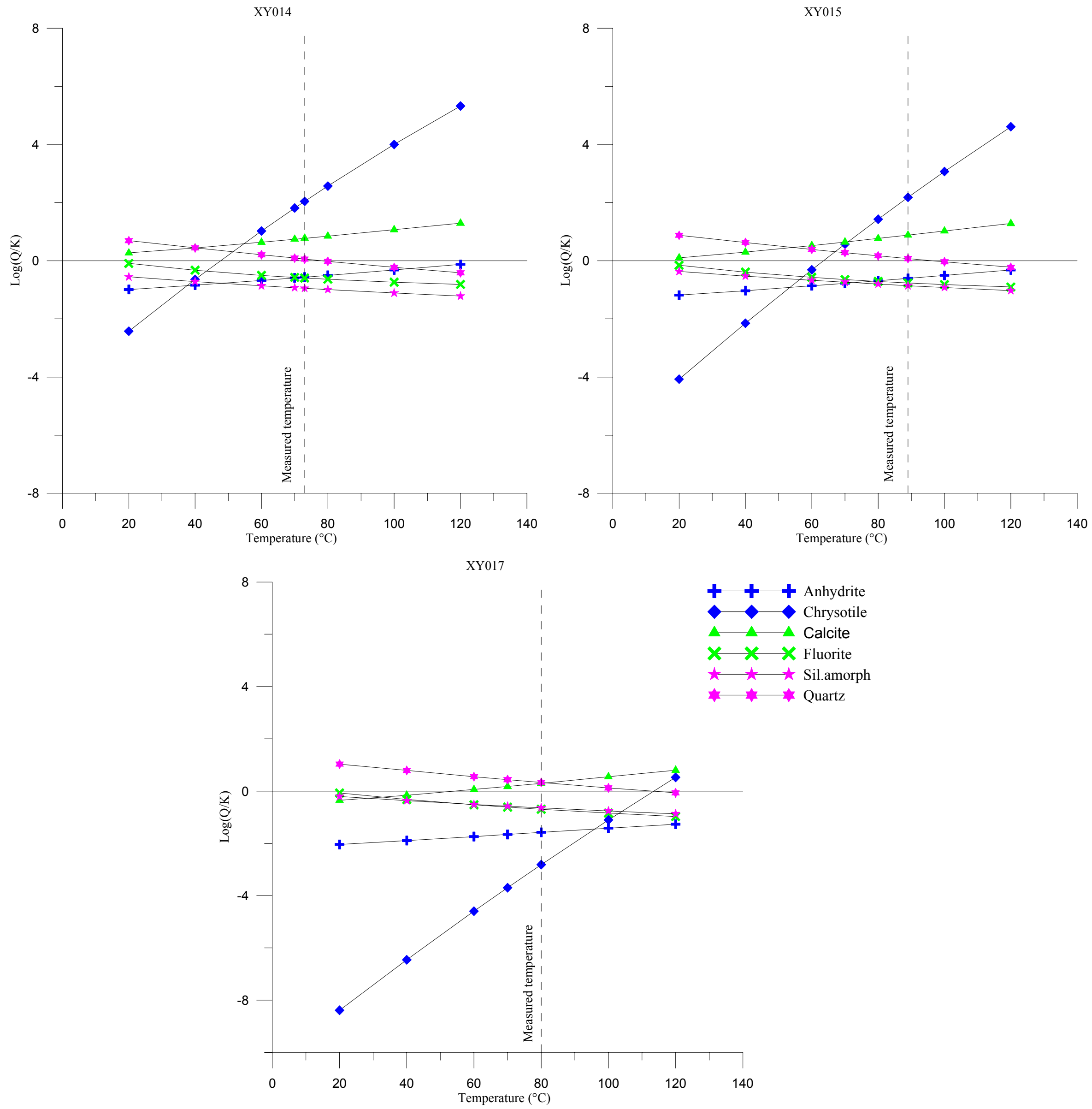

FIGURE 8 continued: Log Q/K diagrams for the Xianyang thermal water samples

3.6 Mixing models

Ascending hot waters may take diverse routes to the surface. They may cool by conduction, boiling, mixing with colder water, or a combination of these processes. When this is the case, partial or complete chemical equilibration may or may not occur after mixing. If chemical equilibrium is established after mixing, the chemical geothermometers indicate temperatures of the mixed water, not the hot water component. Accordingly, whether or not equilibrium is established after mixing, the temperature of the hot water cannot be estimated from a solubility relation unless the mixing is taken into account. Moreover, leaching after mixing tends to dominate the relative cation concentrations. It is unreliable to apply cation geothermometers, except for Na-Li, to mixed waters (Arnórsson, 1985). On the other hand, mixing at deep levels in geothermal reservoirs is likely to be completely masked for reactive constituents through the re-equilibration of these constituents subsequent to the mixing, in which case the application of geothermometers is appropriate for estimating the reservoir temperature. For the above reasons, in some places accurate reservoir temperatures can be given directly by geothermometers such as silica, Na/K, and Na-K-Ca. In other places, mixing models are more appropriate for estimating temperatures of reservoirs deep in the system (Fournier, 1977). However, it should be pointed out that mixing models should not be applied unless there is independent evidence for mixing.

3.6.1 Evidence of mixing

According to the discussion above, there are some indications of mixing in the studied area. Firstly, there is not an agreement between different geothermometers. Silica geothermometer temperatures are lower than the Na-K-Ca temperatures. Secondly, the mineral equilibria diagrams show no clear intersection to the zero saturation index by any group of minerals at a particular temperature.

The Schoeller diagram, in which logarithmic values are used, is an effective tool for showing the mixing of different waters. The log concentration of each constituent for each sample is connected with a line. The effect of mixing with dilute water is to move the line representing an analysis vertically without changing its shape (Truesdell, 1991).

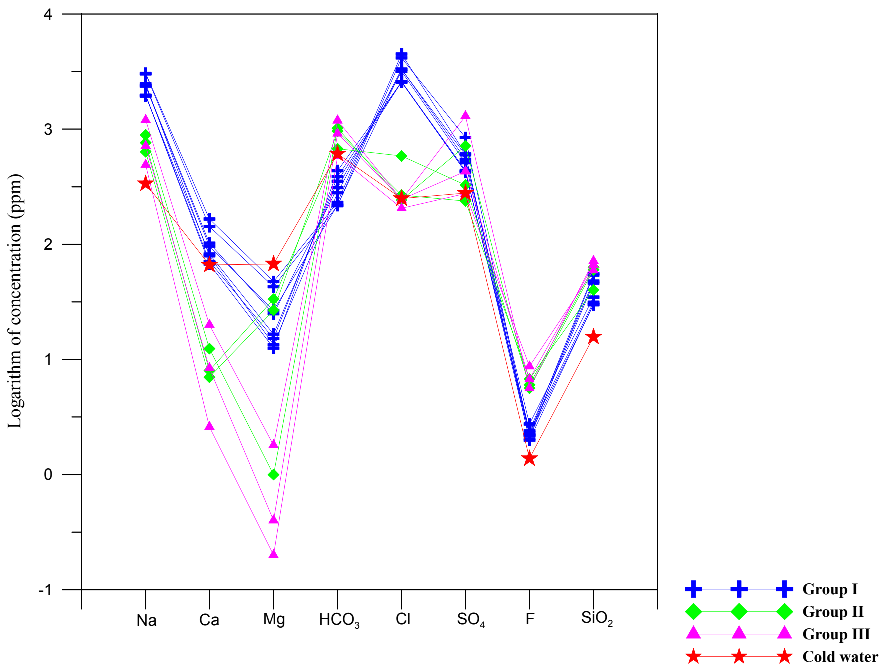

FIGURE 9: Schoeller diagram for the Xianyang thermal water samples

Figure 9 shows a similar trend for the cold and thermal waters plotted in the Schoeller diagram. The variable concentration of magnesium and silica indicates some mixing with cold water. The application of mixing models to estimate reservoir temperatures in Xianyang geothermal field will possibly result in a better understanding of the processes that may take place within the geothermal system.

3.6.2 Mixing models

Although mineral exchange and solution reactions tend to re-equilibrate upon cooling, these reactions are much slower at lower temperatures, and at the same time mixing may reduce temperatures rapidly enough so that the initial, high-temperature equilibrium compositions are frozen in. This principle is employed in mixing models in which the temperature and chemistry of mixed waters are used to calculate the temperature of thermal water before mixing. Under this principle, dissolved silica concentration versus enthalpy can be applied to determine the temperature of the hot water component.

Truesdell and Fournier (1977) proposed a simpler model to estimate the temperature of the deep hot water component, which is a plot of dissolved silica vs. the enthalpy of liquid water. Since the combined heat contents of two waters at different temperatures are conserved when waters are mixed, but the combined temperatures are not, the enthalpy is used as a coordinate rather than the temperature. This model is based on the assumption that no conductive cooling occurred after mixing. If the mixed water cooled conductively after mixing, the calculated temperature of the hot water component would be too high. It is also assumed that no further silica solution and deposition took

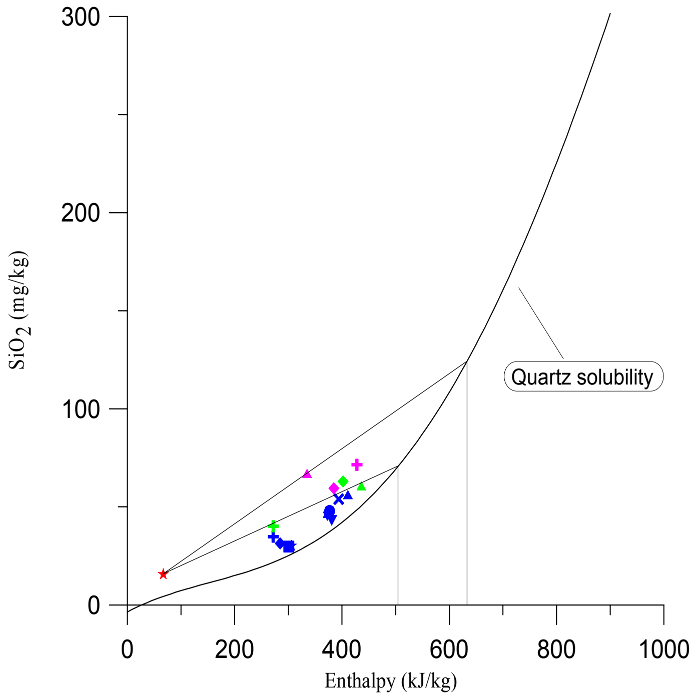

FIGURE 10: SiO_2-enthalpy mixing model for Xianyang thermal water samples

place before or after mixing.

Quartz is believed to control the silica solubility of the geothermal water from Xiayang geothermal system. A silica-enthalpy mixing model was applied to the data, assuming no stream loss. The mixing member, a cold water sample with a silica concentration of 15.7 mg/l and a temperature of 16°C was taken from a Sanppu well. As is seen in Figure 10, some plotted samples tend to cluster at one point, very close to the quartz solubility line. These samples are not appropriate for the estimation of the reservoir temperature. Two lines of mixing are drawn, according to the distribution of the other data points. The upper line between the cold water and the mixed thermal water intersects the quartz solubility curve where enthalpy is approximately equal to 630 kJ/kg, corresponds to the estimated reservoir temperature, 150°C. The lower one, which takes into consideration the remaining points, gives an estimated temperature of 120°C. These temperature estimations are similar to the results from the quartz and Na/K geothermometers, which may explain why the mixing was not obvious and why the mixing model failed to give very conclusive results in the Xianyang geothermal area.

4. EXPLORATION, DEVELOPMENT AND UTILIZATION OF GEOTHERMAL RESOURCES

4.1 Geothermal development and utilization

Geothermal use in Guanzhong basin can be traced back thousands of years. Historically, natural geothermal springs were mainly used for washing and bathing purposes. The oldest pool called Huaqing used by the imperial family as a health spa in ancient times, has become one of the most famous tourist places in Xi'an. Geothermal exploration, including geological and geophysical surveys, started in Xianyang only in the middle of 1980s. At present, the identified geothermal potential is over 10.43×10^{14} cal. In 1993, the first geothermal well was drilled in Xingping. It is 1564 m deep and the temperature of the water reached 60°C. Water from the Xianyang geothermal field is distributed to the cities of Xianyang and Xingping, and the towns of Wugong, Liquan and Sanyuan. The thermal water is used directly for space heating during wintertime and balneological purposes as well as for hot tap water. There are three swimming pools and two spa centres within the distribution system, serving over 20,000 people in 2004. Geothermal production has been steadily increasing in recent years, and from 1993 to 2004 24 geothermal wells were drilled in the area. In 2004, cumulative production amounted to 12 million m^3 and usage in 2004 alone reached about 2 million m^3. Although space heating and tourism are today the main uses of geothermal water, there will possibly be further development of direct uses of the resource in the future (Zhang B, 2005).

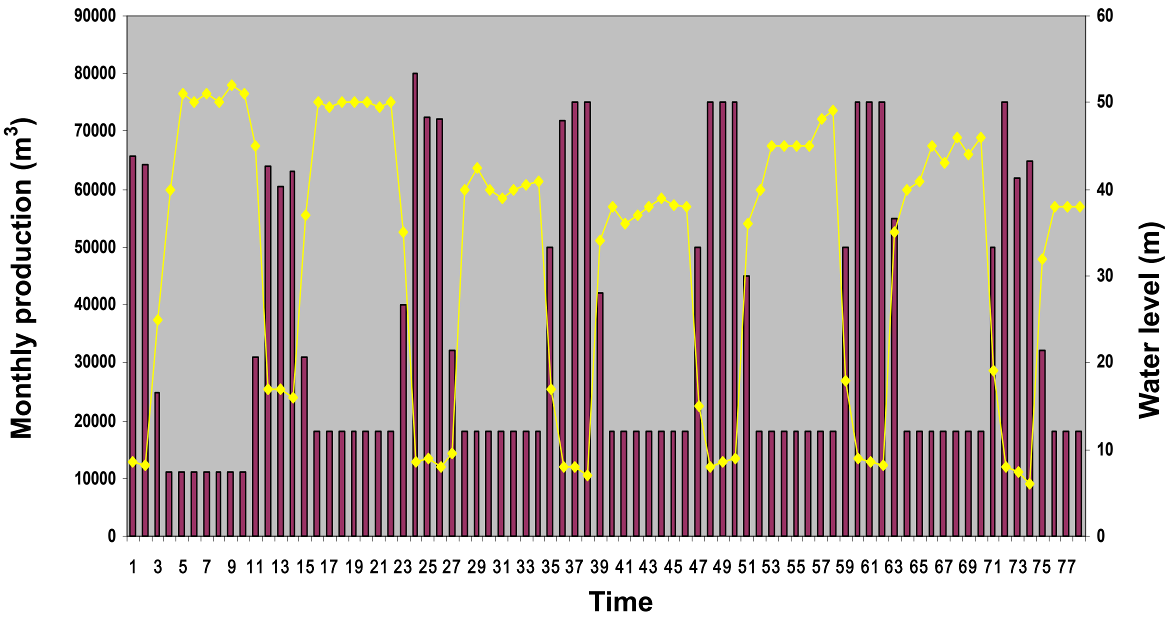

FIGURE 11: Changes in monthly production and water level in Xianyang geothermal field

4.2 Geothermal monitoring

With commercial and large-scale exploration, geothermal resource management appears to be more and more important and careful monitoring is an essential component of any management program. The water level of well XY010, which is located near the North Wei River fault, has been monitored since 1999. Figure 11 shows water level changes in relation to the amount of water produced. During the winter heating period, from November to March, the production increases and water level drops. During the summer when production is at a minimum, the water level rises again. The water level was lower during the summer of 2004 than in 1999, indicating lower pressure in the reservoir.

The estimation of different geothermometers and measured temperature of three wells located near the North Wei river fault are shown in Table 5, for the year drilled (1998 or 1999) and in 2005, respectively. Little or no changes were seen in the measured temperatures but significant changes were found in the estimated quartz and Na/K geothermometer values for wells XY012 and XY014. Values calculated using the quartz geothermometer indicate the temperature in 2005 to be 10°C lower than in 1998/1999 but estimations based on the Na/K geothermometer suggested the reservoir temperature to be 10°C higher in 2005. Further investigation is clearly needed, but this is possibly the effect of mixing of geothermal water in different layers in the reservoir.

TABLE 5: Measured and geothermometer temperatures for the thermal waters from three wells in the Xianyang geothermal field

	XY011		XY012		XY014	
	1998	**2005**	**1998**	**2005**	**1999**	**2005**
T_{mea}	98	98	92	91	74	73
T_{qtz}	106	105	103	93	89	79
$T_{Na/K(1979)}$	109	114	98	108	99	104
T_{K-Mg}	67	68	64	65	63	64

4.3 Environmental benefits

During the four month heating season, extreme temperatures can go as low as -18°C in winter in Xianyang. Until now, the city has mainly relied on fossil fuel as a source of energy. By the end of 2000, the use of fossil fuel resulted in the release of 3500 tons of dust into the atmosphere, about 4000 tons of SO_2 and about 5000 tons of flying ash. Compared to fossil fuel, geothermal energy has obvious environmental advantages. By using geothermal energy for district heating and domestic hot water, air pollution can be reduced. Based on geothermal water production of 12 million m^3, the environmental benefits are estimated in Table 6 (Xing et al., 2005).

Table 6: Environmental benefit assessment of geothermal resources in Xianyang

Time (year)	**Geothermal water production (10^3 m^3)**	**Reduced raw use of coal (10^4 tons)**	**Reduced exhaust emission (tons)**	**Reduced fly ash (tons)**	**Reduced ash (tons)**
2020	11800	14.7	14300	1470	22125

5. SUMMARY AND CONCLUSIONS

- The Xianyang geothermal field has been utilized since 1994 for space heating, tourism and bathing purposes. Over a 10 year period, 1994 to 2004, 24 wells were drilled with the cumulative production amounting to 12 million m^3.
- Water samples from 14 wells were analyzed and divided into three groups according to their distance from the North Wei River Fault. Based upon chemical composition, they were classified as chlorine and carbonate waters, the former from wells near the fault and the latter from wells south of the fault.
- Estimations of subsurface temperatures with quartz- and Na/K-geothermometers predict temperatures in the range of 75-118°C, similar to measured wellhead temperatures.
- The Scoeller diagram clearly shows a great variation of magnesium and silica content of the water but after application of a mixing model, it was concluded that mixing with colder water was not obvious.
- The application of saturation state of the water showed that the geothermal water is not in equilibrium with hydrothermal minerals tested at the measured temperature. The chemical analyses suffered from a lack of aluminum measurements and therefore there was a limited choice of minerals to be tested. Most samples showed a scaling potential for calcite and magnesium silicates, especially if heated, but no scaling problems have been reported at the Xianyang field to date.
- Monitoring of water levels and chemical content showed that there are possibly signs that the geothermal system is affected by increased utilization. Comparison of geothermometer estimates for samples from wells XY012 and XY014 shows that there have been changes in the chemical content of the fluid without changes in the measured wellhead temperatures.
- Monitoring of water levels and further studies of the chemical composition are needed to contribute to a sustainable use of the geothermal reservoir in Xianyang.

ACKNOWLEDGEMENTS

I would like to express my gratitude to Dr. Ingvar B. Fridleifsson, director of the UNU Geothermal Training Programme and Mr. Lúdvík S. Georgsson, deputy director, for giving me the great opportunity to attend this special training and also for their generous advice and assistance. I would also like to thank Mrs. Gudrún Bjarnadóttir and Ms. Thórhildur Ísberg for their kindness and efficient help during the training.

My deepest thanks go to Steinunn Hauksdóttir, my adviser, for her patient instruction, invaluable help and friendliness during the preparation of the report. I also want to express my gratitude to Dr. Halldór Ármannsson for his great help and for sharing his experience and knowledge. I convey my good wishes to all the lecturers and staff members of Orkustofnun and ISOR.

I wish to express my sincere gratitude to Mr. Bian Junjiang, Mr. Ji Weimin, Mr. Yangzhen and Mr. Hewei for making it possible for me to participate in this training. I am greatly indebted to my company and I express my thanks to the entire CGC Construction Company staff members. Deepest thanks to Mr. Huangshiyi and Dr. Liu Jiurong for recommending me for this training. In addition, special thanks to the Bureau of Land & Natural Resources in Xianyang for granting the permission to use their data. I also want to thank the UNU Fellows of 2006 for our unforgettable relationship.

Finally, I am deeply grateful to my parents and friends for their love and support during these six months.

REFERENCES

Ármannsson, H., 2005: *Observation on samples from five geothermal wells in Xianyang.* Iceland GeoSurvey - ÍSOR, Reykjavík, report, 6 pp.

Arnórsson, S., 1985: The use of mixing models and chemical geothermometers for estimating underground temperature in geothermal systems. *J. Volc. Geotherm. Res., 23,* 299-335.

Arnórsson, S. (ed.), 2000a: *Isotopic and chemical techniques in geothermal exploration, development and use. Strategy in geothermal exploration, development and production.* International Atomic Energy Agency, Vienna, 351 pp.

Arnórsson, S., 2000b: The quartz and Na/K geothermometers. I. New thermodynamic calibration. *Proceedings of the World Geothermal Congress 2000, Kyushu-Tohoku, Japan,* 929-934.

Arnórsson, S., Gunnlaugsson, E., Svavarsson, H., 1983a: The chemistry of geothermometry of geothermal waters in Iceland II: Mineral equilibria and independent variables controlling water compositions. *Geochim. Cosmochim. Acta, 47,* 547-566.

Arnórsson, S., Gunnlaugsson, E., and Svavarsson, H., 1983b: The chemistry of geothermal waters in Iceland III. Chemical geothermometry in geothermal investigations. *Geochim. Cosmochim. Acta, 47*, 567-577.

Arnórsson, S., Sigurdsson, S., and Svavarsson, H., 1982: The chemistry of geothermal waters in Iceland I. Calculation of aqueous speciation from 0°C to 370°C. *Geochim. Cosmochim. Acta, 46,* 1513-1532.

Axelsson, G. and Ármannsson, H., 2005: *Characteristics and potential of geothermal resources in Xianyang, Shaanxi province, China*. ÍSOR, Reykjavík, report ÍSOR2006/127, 36 pp.

Bjarnason, J.Ö., 1994: *The speciation program WATCH, version 2.1.* Orkustofnun, Reykjavík, 7 pp.

Fouillac, C., and Michard, G., 1981: Sodium/lithium ratios in water applied to geothermometry of geothermal reservoirs. *Geothermics, 10,* 55-70.

Fournier, R.O., 1977: Chemical geothermometers and mixing model for geothermal systems. *Geothermics, 5,* 41-50.

Fournier, R.O., 1979: A revised equation for Na-K geothermometer. *Geoth. Res. Council, Trans., 3,* 221-224.

Fournier, R.O., 1989: *Lectures on geochemical interpretation of hydrothermal waters*. UNU-GTP, Iceland, report 10, 73 pp.

Fournier, R.O., and Truesdell, A.H., 1973: An empirical Na-K-Ca geothermometer for natural waters. *Geochim. Cosmochim. Acta*, *37*, 1255-1275.

Fournier, R.O., and Potter, R.W. II, 1982: A revised and expanded silica (quartz) geothermometer. *Geotherm. Resourc. Counc. Bull., 11-10,* 3-12.

Giggenbach, W.F., 1988: Geothermal solute equilibria. Derivation of Na-K-Mg-Ca geoindicators. *Geochim. Cosmochim. Acta, 52*, 2749-2765.

Giggenbach, W.F., 1991: Chemical techniques in geothermal exploration. In: D'Amore, F. (coordinator), *Application of geochemistry in geothermal reservoir development*. UNITAR/UNDP publication, Rome, 119-142.

Qin D., Turner, J.V. and Pang, Z. 2005: Hydrochemistry and groundwater circulation in the Xi'an geothermal field, China. *Geothermics, 34,* 471-494.

Reed, M., and Spycher, 1984: Calculation of pH and mineral equilibria in hydrothermal waters with application to geothermometry and studies of boiling and dilution, *Geochim. Cosmochim. Acta, 48*, 1479-1490.

Tao, S., 1995. The formation of geothermal water near Xi'an (in Chinese). *Hydrogeol. Eng. Geo., 5,* 6-11.

Tian, C., and Zheng, X., 1995. *Hydrogeology in the Guanzhong Basin.* Xi'an Scientific Publishing House, 2151-2166.

Tole, M.P., Ármannsson, H., Pang Z., and Arnórsson, S., 1993: Fluid/mineral equilibrium calculations for geothermal fluids and chemical geothermometry. *Geothermics, 22*, 17-37.

Truesdell, A.H., 1991: Effects of physical processes on geothermal fluids. In: D'Amore, F. (coordinator), *Application of geochemistry in geothermal reservoir development.* UNITAR/UNDP publication, Rome, 71-92.

Truesdell, A.H., and Fournier, R.O., 1977: Procedure for estimating the temperature of a hot water component in a mixed water using a plot of dissolved silica vs. enthalpy. *U.S. Geol. Survey J. Res., 5,* 49-52.

Xie Zh., 1998: Analysis for the geotectonic setting of underground hot water in the Weihe Fault depression (in Chinese). *Geology of Shaanxi, 16-2*.

Xing X., Sun J., Jia, J., Tian H., H C., Luo D., and Liu Q., 2005: *Report of geothermal resources exploration, Xianyang in Shaanxi province* (in Chinese). Xianyang Bureau of Land and Natural Resources, report, 77 pp.

Zhang B., 2005: Geothermal resources in China. *Proceedings of the World Geothermal Congress 2005, Antalya, Turkey*, CD, 3 pp.